Impact of Zero-Dispersion Wavelength Fluctuations in a Coupled Dual-Core Fiber Optical Parametric Amplifier

Vitor Ribeiro, Minji Shi and Auro M. Perego

***Abstract*—We have studied the impact of zero-dispersion wavelength (ZDW) fluctuations in coupled dual-core fiber optical parametric amplifiers (FOPAs) and compared it to the single-core single-pump FOPA. We have designed a Monte Carlo model, that simulates a multidimensional Ornstein–Uhlenbeck process, describing accurately ZDW fluctuations in single and multicore fibers. In order to validate our results we have developed an analytical model, based on Taylor expansion of the average gain and successfully compared both models, with experimental results published in the literature. We have found that a significant reduction of the impact of ZDW fluctuations can be obtained in dual-core FOPAs compared to single-core ones.**

***Index Terms*—Fiber optical parametric amplifiers, Coupled-core fibers, fiber supermodes, Zero-dispersion wavelength fluctuations.**

I. Introduction

Fiber optical parametric amplifiers (FOPAs) offer some attractive features, such as potential for wide-bandwidth, low noise figures below 3 dB, when operated in phase-sensitive mode [1] and fast nonlinear response suitable for burst-mode amplification [2], [3]. However some physical effects determined by either the physics of third-order nonlinear response of the fiber, such as stimulated Brillouin scattering (SBS) that prevents the launch of strong pump power, or by fiber imperfections introduced during its manufacturing, limit the noise figure, the maximum attainable gain and the bandwidth (BW) of the FOPA.

The impact of zero-dispersion wavelength (ZDW) fluctuations has been mostly treated at the theoretical level [4]–[8]. However few works address their impact experimentally. Nonetheless ZDW fluctuations profile were already measured in a lab environment and models were devised in order to compare and assess their impact on the gain spectrum of the FOPA device [9], [10].

The study of parameter fluctuations in multicore fibers indicate that the amplitude of fluctuations of the core radius is approximately 2 % of the nominal core radius and that fluctuations in different cores are not independent [11], i.e. they have some level of correlation. These core radius fluctuations are a result of fiber imperfections and come as a result of the manufacturing process, leading to fluctuations of propagation constants along the longitudinal dimension of the fiber. ZDW fluctuations have been modeled as exponentially correlated along the longitudinal dimension of the fiber [4], which has been verified experimentally too [12]. In the case of the single-core single-pump FOPA, Karlsson [4] assumed that the statistics of ZDW fluctuations along the longitudinal dimension of the fiber is an Ornstein–Uhlenbeck (OU) process. We will show in this paper that this also applies to the scenario of a dual-core (DC)-FOPA by applying a multidimensional OU process. In [8] the one dimensional OU process, was implemented numerically, however Model I of [8] is just usable if ZDW fluctuations in every interacting mode of the fiber, no matter if the interacting mode is in space or frequency, are perfectly correlated. This is true for single-core single-pump FOPA, i.e. for signal and idler modes, but may not be true for coupled DC-FOPA, where the spatial modes may not have the same ZDW fluctuations. This is because model I of [8], requires that the distinct matrices that model each segment dz of the fiber commute, i.e, if A and B, are two of those matrices, the following equality $e^{A+B} = e^A e^B$, is true, if and only if, A and B commute which in the case studied in this paper is only true, when ZDW fluctuations in both cores are perfectly correlated. Model I of [8] overestimates performance when ZDW fluctuations are not perfectly correlated and may mislead into incorrect results. Therefore in this paper we use model II of [8] and extend it to the case of coupled DC-FOPA, using a multidimensional OU process.

Therefore in this paper we model and study ZDW fluctuations impact on recently proposed coupled DC-FOPA [13]–[20]. Coupled DC-FOPAs present a set of features that can make them attractive for future fiber optical communication networks, such as exponential and flat gain profile [13], potential to provide 0 dB noise figure [14], without the requirement to generate frequency converted copies of the signal, by nonlinear frequency translation techniques (usually mentioned as copier stage). In this paper we have used an extension of the one dimensional case to the multidimensional case of model II of [8] in order to study the impact of ZDW fluctuations on coupled DC-FOPA using Monte Carlo simulations. We also developed a theoretical model, using a Taylor expansion of the average gain to compare with Monte Carlo simulations and experiments available in the literature and performed for single-core single-pump FOPA [9]. We have furthermore compared performances against ZDW fluctuations of DC-FOPA and single-core single-pump FOPA.

This paper is organized as follows. In section II we develop the theoretical formalism to describe the DC-FOPA and we

Vitor Ribeiro, Minji Shi and Auro M. Perego are with Aston Institute of Photonic Technologies, Aston University, B4 7ET, Birmingham, UK Vitor Ribeiro is now with Kets Quantum Security Ltd. BS15 4PJ Bristol, UK (vitor.ribeiro@kets-quantum.com)

introduce the Monte Carlo simulation model and the analytical model. In section III we experimentally validate the models developed in Section II. In section IV we assess the performance of DC-FOPA against ZDW fluctuations and compare it with single-core single-pump FOPA. In Section IV we present the conclusions.

II. Theoretical and Analytical Background

A. General theoretical formalism

We consider a DC fiber, where the electric fields slowly varying envelope evolution along the two evanescently coupled cores is described by two coupled nonlinear Schrödinger equations (NLSEs) [21]

$$\begin{aligned}\frac{\partial U_1}{\partial z} &= i\sum_{n=0}^{\infty} i^n \frac{\beta_{n_1}(z)}{n!}\frac{\partial^n U_1}{\partial t^n} + i\gamma U_1|U_1|^2 - \frac{\alpha}{2}U_1 + iCU_2 \\ \frac{\partial U_2}{\partial z} &= i\sum_{n=0}^{\infty} i^n \frac{\beta_{n_2}(z)}{n!}\frac{\partial^n U_2}{\partial t^n} + i\gamma U_2|U_2|^2 - \frac{\alpha}{2}U_2 + iCU_1.\end{aligned} \tag{1}$$

Here $U_{1,2}$ are the two field amplitudes defined in a temporal reference in the lab frame of coordinate t and evolving along spatial coordinate z. γ and α are nonlinearity and loss coefficient respectively. $\beta_{n1,2}(z) = \frac{\partial^n \beta_{1,2}}{\partial \omega^n}|_{\omega=\omega_0}$ are the n-th order derivatives of the z-dependent propagation constants $\beta_{1,2}$, with respect to frequency ω and evaluated at the carrier frequency ω_0. In this paper we assume C to be constant and independent of wavelength and $\alpha = 0$, which holds for fibers but not for integrated waveguides. To note that in this paper we will restrict our analysis to $n <= 4$, neglecting all the other higher order terms of the dispersion. Recently a first description of a parametric amplifier based on coupled core fibers has been developed obtaining an analytical solution for the gain [13], [14].

Starting from Eqs.1 it is possible to derive the coupled evolution equations for the pump (u_{p_1}, u_{p_2}), signal (u_{s_1}, u_{s_2}), and idler (u_{i_1}, u_{i_2}) wave amplitudes, where the subscripts $1, 2$ refer to the two cores respectively and the subscripts p, s, i refer to quantities connected to pump, signal and idler waves:

$$\begin{aligned}\frac{\partial u_{p_1}}{\partial z} &= iu_{p_1}\left(\beta_{p_1}(z) + \gamma(2P_1 - |u_{p_1}|^2)\right) + i\gamma 2u^*_{p_1}u_{s_1}u_{i_1} \\ &\quad + iCu_{p_2} \\ \frac{\partial u_{s_1}}{\partial z} &= iu_{s_1}\left(\beta_{s_1}(z) + \gamma(2P_1 - |u_{s_1}|^2)\right) + i\gamma u^2_{p_1}u^*_{i_1} \\ &\quad + iCu_{s_2} \\ \frac{\partial u_{i_1}}{\partial z} &= iu_{i_1}\left(\beta_{i_1}(z) + \gamma(2P_1 - |u_{i_1}|^2)\right) + i\gamma u^2_{p_1}u^*_{s_1} \\ &\quad + iCu_{i_2}\end{aligned} \tag{2}$$

where the equations for the second core can be obtained by exchanging subscripts 1 and 2. Here $P_1 = |u_{p_1}|^2 + |u_{s_1}|^2 + |u_{i_1}|^2$, $P_2 = |u_{p_2}|^2 + |u_{s_2}|^2 + |u_{i_2}|^2$ and the $\beta_{w_{1,2}}(z)|_{w=s,i}$ coefficients describe the propagation constants for cores 1 and 2, respectively. We now assume that both cores are pumped with the same input pump power such that $P_{p1} + P_{p2} = P_p$ and consider that $P_p/2 >> |u_{s,i}|^2$, corresponding to the fact that signals and idlers do not deplete the pump waves. Under this approximation the pump amplitudes admit the following solutions [13], [14]:

$$u_{p_{1,2}}(z) = \sqrt{\frac{P_p}{2}}e^{i\phi_0 + i\int_0^z \beta_{p_{1,2}}(z')dz' + i\frac{P_p\gamma}{2}z + iCz}$$

where ϕ_0 is a locked phase factor for the pumps. We furthermore write the sidebands amplitudes in the two cores as a function of the new amplitudes $e_{s_1}(z), e_{i_1}(z), e_{s_2}(z), e_{i_2}(z)$ [13], [14]

$$\begin{aligned}e_{s_1,i_1,s_2,i_2}(z) &= u_{s_1,i_1,s_2,i_2}(z) \times \\ &\times e^{-i\int_0^z \beta_{s_1,i_1,s_2,i_2}(z')dz' - i\frac{P_p\gamma}{2}z} \times e^{i\int_0^z \frac{\Delta\beta_{1,2}(z')}{2}dz' - iCz}\end{aligned} \tag{3}$$

where $\Delta\beta_{1,2}(z) = \beta_{s_{1,2}}(z) + \beta_{i_{1,2}}(z) - 2\beta_{p_{1,2}}(z)$ is the linear mismatch. Using the above mentioned approximations and definitions we can write the set of linear coupled differential equations ruling the evolution of $\vec{E}(z) = \left(e_{s_1}(z), e^*_{i_1}(z), e_{s_2}(z), e^*_{i_2}(z)\right)^T$ in matrix form as:

$$\frac{\partial \vec{E}(z)}{\partial z} = M(z)\vec{E}(z) \tag{4}$$

where T is the transpose operator and

$$\begin{aligned}M(z) &= \begin{pmatrix} ik_1(z) & i\frac{\gamma P_p}{2} & iC & 0 \\ -i\frac{\gamma P_p}{2} & -ik_1(z) & 0 & -iC \\ iC & 0 & ik_2(z) & i\frac{\gamma P_p}{2} \\ 0 & -iC & -i\frac{\gamma P_p}{2} & -ik_2(z)\end{pmatrix} = \\ &= \begin{pmatrix} M_1 & M_c \\ M_c & M_2\end{pmatrix}.\end{aligned} \tag{5}$$

Here $k_{1,2}(z) = \frac{P_p\gamma}{2} + \frac{\Delta\beta_{1,2}(z)}{2} - C$ is the total mismatch parameter for cores 1,2 accounting for nonlinear, linear and coupling contribution. $M_{1,2}$ and M_c are the 2×2 diagonal and off-diagonal sub-matrices of $M(z)$, respectively. We can write $k_{1,2}(z)$ as a function of the ZDW fluctuations in the following manner, $k_1(z) = \frac{P_p\gamma}{2} + \frac{(2\pi c)^3\beta_3}{2\lambda^6_{p_1}}\Delta\lambda_1\lambda^2 + \frac{(2\pi c)^4\beta_4}{24\lambda^8_{p_1}}\lambda^4$ and $k_2(z) = \frac{P_p\gamma}{2} + \frac{(2\pi c)^3\beta_3}{2\lambda^6_{p_2}}\Delta\lambda_2\lambda^2 + \frac{(2\pi c)^4\beta_4}{24\lambda^8_{p_2}}\lambda^4$. The parameter c is the speed of light, λ is the wavelength shift of the signal with respect to the pump wavelengths $\lambda_{p_{1,2}}$, $\beta_{3,4}$ are the third and fourth order dispersion parameter at the pump wavelengths, $\Delta\lambda_{1,2}(z) = \langle\lambda_{0_{1,2}}\rangle - \lambda_{p_{1,2}} + \delta\lambda_{0_{1,2}}(z)$ is the difference between the average $\langle\lambda_{0_{1,2}}\rangle$ of the ZDW, the wavelength of the pump and the longitudinal fluctuations of the ZDW in cores 1 and 2 $\delta\lambda_{0_{1,2}}(z)$, respectively. For the sake of simplicity we will restrict our cases of study to $\lambda_{p_1} = \lambda_{p_2} = \lambda_p$ and $\langle\lambda_{0_1}\rangle = \langle\lambda_{0_2}\rangle = \langle\lambda_0\rangle$. However (4) can be solved to account when this does not occur. We can rewrite $k_{1,2}(z) = \langle k_{1,2}\rangle + \Delta_{k_{1,2}}(z)$, which is the result of the sum of an average and independent of z phase-mismatch parameter, i.e., $\langle k_{1,2}\rangle$ and a varying part which is a function of the ZDW fluctuations, i.e. $\Delta_{k_{1,2}}(z)$.

B. Monte Carlo simulation model

The numerical model uses a 4^{th} order Runge-Kutta (RK4) solver to calculate the solution of (4). To note that an implementation of a one dimensional exponentially correlated OU

process was performed in [8] and the general description can be found in [22]. For 2 dimensions, we generally have to define a multivariate OU process, with $\delta\lambda_0 = (\delta\lambda_{0_1}, \delta\lambda_{0_2})^T$, where [23, Eq. 7],

$$\Theta(z - z') = \langle \delta\lambda_0(z)\delta\lambda_0(z')^T \rangle = \Theta(0)\Lambda \tag{6}$$

is the z dependent correlation function, with the normal bivariate covariance matrix given by

$$\Theta(0) = \begin{pmatrix} \sigma_{\lambda_1}^2 & \rho\sigma_{\lambda_1}\sigma_{\lambda_2} \\ \rho\sigma_{\lambda_1}\sigma_{\lambda_2} & \sigma_{\lambda_2}^2 \end{pmatrix} \tag{7}$$

and $\Lambda = e^{-\theta|\Delta z|}$, where $\Delta z = z - z'$ and $\rho = \frac{E\left[\left(\delta\lambda_{0_1} - E[\delta\lambda_{0_1}]\right)\left(\delta\lambda_{0_2} - E[\delta\lambda_{0_2}]\right)\right]}{\sigma_{\lambda_1}\sigma_{\lambda_2}}$, is the Pearson correlation coefficient, where E is the average operator, σ_{λ_1} and σ_{λ_2} are the standard deviations of $\delta\lambda_{0_1}$ and $\delta\lambda_{0_2}$, over the full length of the fiber, respectively, and

$$\theta = \begin{pmatrix} 1/L_{c_1} & 0 \\ 0 & 1/L_{c_2} \end{pmatrix}. \tag{8}$$

Here we assume the off-diagonal terms of θ are zero. In this study, we restrict to the cases, where $L_{c_1} = L_{c_2}$. This has been followed in other models using exponentially correlated fluctuations in multicore fibers with the aim of estimating crosstalk impact too [24]–[26]. The matrix θ is the regression rate matrix of an OU process [23]. The algorithm has the following steps for each of the $N = 1000$ realizations of the fiber,

1) initialize
$$\delta\lambda_0(z = 0) = \begin{pmatrix} \mathcal{N}(0,1) \\ \mathcal{N}(0,1) \end{pmatrix}, \tag{9}$$
where $\mathcal{N}(0,1)$ is a normally distributed value with mean 0 and standard deviation equal to 1. Set $\Delta z = \min\left[L_{c_1}/250, L_{c_2}/250, L/1000\right]$, where L is the total length of the fiber, in order that $\Delta z/\min\left(L_{c_1}, L_{c_2}\right) \ll 1$ [23].
2) for the whole length of the fiber simulate the exponentially correlated ZDW fluctuations in the following recursive way [8], [22], [27], [23, Eq. 21],
$$\delta\lambda_0(z+\Delta z) = \Lambda\delta\lambda_0(z) + \sqrt{I - \Lambda^2}\begin{pmatrix} \mathcal{N}(0,1) \\ \mathcal{N}(0,1) \end{pmatrix}, \tag{10}$$
where I is the identity matrix. The interpretation of this equation is quite simple. If ZDW fluctuation at length z is decorrelated with fluctuation at length $z+\Delta z$, then in order to correlate them we need to have the exponential correlation factor Λ. This is similar to what is done in order to correlate two decorrelated random processes by a Pearson correlation coefficient.
3) a check need to be done to guarantee that fluctuations in core 1 are not ρ correlated with fluctuations in core 2 and guarantee that both become $\mathcal{N}(0,1)$, i.e.,$\delta\lambda_0 = \left(\delta\lambda_0 - \left(\mu'_{\lambda_1}, \mu'_{\lambda_2}\right)^T\right) \oslash \left(\sigma'_{\lambda_1}, \sigma'_{\lambda_2}\right)^T$, where $\mu'_{\lambda_{1,2}}$ and $\sigma'_{1,2}$ are the means and standard deviations of $\delta\lambda_{0_{1,2}}$,respectively, resultant from the calculation of (10) and $\oslash$ is the element-wise vector/matrix Hadamard division [28].
4) decompose $\Theta(0)$, using Cholesky decomposition, i.e., $\Theta(0) = \Gamma\Gamma^T$, where
$$\Gamma = \begin{pmatrix} \sigma_{\lambda_1} & 0 \\ \rho\sigma_{\lambda_2} & \sqrt{1-\rho^2}\sigma_{\lambda_2} \end{pmatrix} \tag{11}$$
and for all the length of the vector we calculate $D_{\delta\lambda_0}(z) = \delta\lambda_0(z + \Delta z) - \delta\lambda_0(z)$, generating 2 decorrelated Wiener processes increments [29].
5) Finally in order to correlate in amplitude the fluctuations of the ZDW in cores 1 and 2 by the Pearson coefficient ρ, we use matrix Γ [29].
$$\delta\lambda_0(z + \Delta z) = \delta\lambda_0(z) + \Gamma D_{\delta\lambda_0}(z). \tag{12}$$
To note that we split [23, Eq. 21] in two steps. First, we make the longitudinal correlation along z accordingly to matrix Λ (step 2) and then we correlate the amplitude of the fluctuations (step 5).While (10) could include in a single step the targeted value of the standard deviation of ZDW fluctuations, correlation length and Pearson correlation coefficient as it is suggested by [23, Eq. 21], it is hard to generate these in one single step and with the desired accuracy simultaneously. In order to have the targeted Pearson correlation coefficient with (12), it is strictly necessary to guarantee that the ZDW fluctuations of core 1 and 2, obtained with (10), are completely amplitude decorrelated, i.e. $\rho = 0$. Moreover, $D_{\delta\lambda_0}$ reverses the integration operation started by (10), generating noise with Gaussian statistics. This noise when integrated back generates two amplitude decorrelated processes, with the longitudinal correlation set in (10). This integration is therefore reinstated by (12), but this time with the targeted standard deviation and Pearson correlation coefficient, while preserving the previously set correlation length. This was indeed validated and tested thoroughly during this work.
6) The gain of the system is obtained by solving (4) with a RK4 method and by using $Gain = \frac{\left|e_{s_1}(z) - e_{s_2}(z)\right|^2}{\left|e_{s_1}(0) - e_{s_2}(0)\right|^2}$ [15].

Fig. 1 provides some examples of ZDW fluctuations, obtained using the algorithm above. One can see that the longer the correlation length the smoother the evolution of the ZDW fluctuations becomes, and we show it for several values of the Pearson coefficient ρ. For exponentially correlated random variables, the spectrum of the auto-correlation function is a Lorentzian function which is narrower for larger correlation lengths and therefore will have an impact on the BW of the fiber.

C. Theoretical model

In order to develop an analytical model for the average gain, $M(z)$ is more conveniently written considering super-modes i.e, $\vec{E}_{\pm}(z) = \left(e_{s\pm}(z), u^*_{i\pm}(z)\right)^T = \left(e_{s_1}(z) \pm e_{s_2}(z), e^*_{i1}(z) \pm e^*_{i2}(z)\right)^T$ in that way a super-mode equivalent of (4) and (5) reads as

$$\frac{\partial\vec{E}_{\pm}(z)}{\partial z} = \begin{pmatrix} M_+(z) & M_{12}(z) \\ M_{12}(z) & M_-(z) \end{pmatrix}\vec{E}_{\pm}(z) = M_{SM}(z)\vec{E}_{\pm}(z) \tag{13}$$

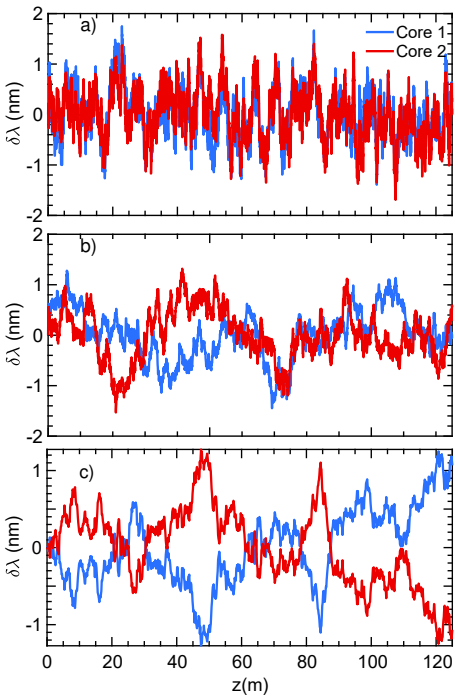

Fig. 1. ZDW fluctuations patterns obtained for different parameters: a) $L_{c_1} = L_{c_2} = 1$ m, $\sigma_{\lambda_1} = \sigma_{\lambda_2} = 0.5$ nm and $\rho = 0.8$, b) $L_{c_1} = L_{c_2} = 10$ m, $\sigma_{\lambda_1} = \sigma_{\lambda_2} = 0.5$ nm and $\rho = 0$, c) $L_{c_1} = L_{c_2} = 40$ m, $\sigma_{\lambda_1} = \sigma_{\lambda_2} = 0.5$ nm and $\rho = -1$.

where $M_{\pm} = \frac{M_1 + M_2}{2} \pm M_c$ and $M_{12} = \frac{M_1 - M_2}{2}$ resulting in the following matrices

$$M_+ = \begin{bmatrix} \mathrm{i}\frac{k_1(z)+k_2(z)}{2} & \mathrm{i}\frac{P_p\gamma}{2} \\ -\mathrm{i}\frac{P_p\gamma}{2} & -\mathrm{i}\frac{k_1(z)+k_2(z)}{2} \end{bmatrix} \quad (14)$$

$$M_- = \begin{bmatrix} -\mathrm{i}2C + \mathrm{i}\frac{k_1(z)+k_2(z)}{2} & \mathrm{i}\frac{P_p\gamma}{2} \\ -\mathrm{i}\frac{P_p\gamma}{2} & \mathrm{i}2C - \mathrm{i}\frac{k_1(z)+k_2(z)}{2} \end{bmatrix}$$

$$M_{12} = \begin{bmatrix} \mathrm{i}\frac{k_1(z)-k_2(z)}{2} & 0 \\ 0 & -\mathrm{i}\frac{k_1(z)-k_2(z)}{2} \end{bmatrix}$$

we note that M_{12} provides the coupling between the super-modes $\vec{E}_+$ and $\vec{E}_-$. In order to reduce the dimensional complexity of the problem, we restrict this study to the input initial conditions proposed in [14] for best noise performance, i.e. $e_{s_1} = -e_{s_2} = e_s$ and $e_{i_1} = e_{i_2} = 0$. We stress that as first demonstrated by Mecozzi [30], this configuration leads to $\vec{E}_+$ being attenuated or squeezed while $\vec{E}_-$ is amplified. Therefore this setup is the spatial analogous of a phase-sensitive frequency degenerate/non-degenerate parametric amplifier [31] and therefore of most interest for this study. This results in the following input vector $\vec{E}_+(0) = (0, 0)$ and $\vec{E}_-(0) = (2e_s, 0)$. A schematic implementation of this super-mode system is shown in [15, Fig. 8]. In order to get the solution of the problem we approximate the solution of (13) by using the following procedure [32]:

$$\vec{E}_{\pm}(z) \approx e^{\int_0^z M_{SM}(z')dz'}\vec{E}_{\pm}(0) = N\vec{E}_{\pm}(0). \quad (15)$$

Here the integral reads

$$\int_0^z M_{SM}(z')dz' = \begin{pmatrix} \mathrm{i}K_+(z) & \mathrm{i}\frac{P_p\gamma}{2} & \mathrm{i}K_-(z) & 0 \\ -\mathrm{i}\frac{P_p\gamma}{2} & -\mathrm{i}K_+(z) & 0 & -\mathrm{i}K_-(z) \\ \mathrm{i}K_-(z) & 0 & -\mathrm{i}2C + \mathrm{i}K_+(z) & \mathrm{i}\frac{P_p\gamma}{2} \\ 0 & -\mathrm{i}K_-(z) & -\mathrm{i}\frac{P_p\gamma}{2} & \mathrm{i}2C - \mathrm{i}K_+(z) \end{pmatrix} z, \quad (16)$$

where $K_{\pm}(z) = \frac{\int_0^z \frac{k_1(z')\pm k_2(z')}{2}dz'}{z}$ and $\Delta\lambda'_{1,2} = \int_0^z \Delta\lambda_{1,2}(z')dz' = \int_0^z \left(\langle\lambda_{0_{1,2}}\rangle - \lambda_{p_{1,2}} + \delta\lambda_{0_{1,2}}(z')\right)dz'$ is a bivariate OU process with variance, [23, Eq. 4], [33, After Eq. 1.3],

$$\Sigma(L,\theta') = \int_0^L e^{-\theta' u}\Gamma\Gamma^T e^{-\theta' u T}du = \frac{1}{2\theta'}\left(\Theta(0) - e^{-\theta' L}\Theta(0)\left(e^{-\theta' L}\right)^T\right). \quad (17)$$

For the particular process of ZDW fluctuations in dual core fibers, the set of parameters $\left(\Sigma', \theta'\right)$ needs to be estimated [23], [33], [34]. We will make a trial solution and further compare it with numerical and experimental results. Therefore we substitute, $\Sigma' = \frac{\Sigma}{m^2}$ and $\theta' = \theta m^2$, where m is the number of dimensions being considered by the problem ($m = 2$ as we have a bivariate OU process).

The gain of the FOPA can be derived from

$$\left|\frac{\vec{E}_-(z)}{\vec{E}_-(0)}\right|^2 = |N_{33}|^2 \quad (18)$$

and

$$G(\Delta\lambda'_1, \Delta\lambda'_2) = N_{33}. \quad (19)$$

Here N_{33} is the element of matrix N at 3rd row and 3rd column and reads

$$N_{33} = \frac{1}{2\varepsilon}\left[\cosh(\xi_1 z)\eta_1 + \frac{\mathrm{i}\sinh(\xi_1 z)}{\xi_1}(\mu+\nu) + \cosh(\xi_2 z)\eta_2 + \frac{\mathrm{i}\sinh(\xi_2 z)}{\xi_2}(\mu-\nu)\right], \quad (20)$$

where

$$\varepsilon = \sqrt{(K_+ - C)^2(K_-^2 + C^2)},\ \mu = (K_+ - 2C)\varepsilon,$$
$$\nu = K_+^2 C + 2C^3 + CK_-^2 - K_+K_-^2 - 3K_+C^2,$$
$$\xi_{1,2} = \sqrt{\gamma^2 P_p^2/4 \pm \varepsilon - (K_+ - C)^2 - K_-^2 - C^2},$$
$$\eta_{1,2} = \varepsilon \pm (K_+C - C^2).$$

In order to estimate theoretically the mean of $G(\Delta\lambda'_1, \Delta\lambda'_2)$, over different random realizations of the fiber i.e., $E[G(\Delta\lambda'_1, \Delta\lambda'_2)]$ we expand $E[G(\Delta\lambda'_1, \Delta\lambda'_2)]$ in a Taylor series [35, Eq. 4.30]

$$E[G(\Delta\lambda'_1, \Delta\lambda'_2)] \approx G(\langle\Delta\lambda'_1\rangle, \langle\Delta\lambda'_2\rangle) + \frac{1}{2!}\sum_{j=1}^{2}\sum_{i=1}^{2}\frac{\partial^2 G(\Delta\lambda'_1, \Delta\lambda'_2)}{\partial\Delta\lambda'_i\partial\Delta\lambda'_j}Cov\left(\Delta\lambda'_i, \Delta\lambda'_j\right)\Big|_{\substack{\Delta\lambda'_1 = \langle\Delta\lambda'_1\rangle \\ \Delta\lambda'_2 = \langle\Delta\lambda'_2\rangle}} + \cdots \quad (21)$$

To note that the odd terms of the Taylor expansion of $E[f(x)]$ are zero [35, Eq. 4.30], for any function of random variables $f(x)$. $Cov\left(\Delta\lambda_i^{'}, \Delta\lambda_j^{'}\right) = \left.\frac{\Sigma^{'}\left(z,\theta^{'}\right)}{L}\right|_{i,j}$, where i and j are the row and column index of $\Sigma^{'}(z,\theta^{'})$. This indicates that the vector of estimated parameters $\left(\Sigma^{'},\theta^{'}\right)$ is normalized by the length L of the fiber in order to account for the impact of the correlation length on the gain spectrum of the FOPA. As an example $Cov\left(\Delta\lambda_n^{'}, \Delta\lambda_n^{'}\right) = \frac{L_{c_n}\sigma_{\lambda_n}}{2m^2}\left(1 - e^{-\frac{2m^2}{L_{c_n}}}\right)\frac{\sigma_{\lambda_n}}{m^2}$. Caution needs to be taken in terms of the units of the variables involved in an OU process. The differential equation of an OU process [23, Eq. 1], in the case $\delta\lambda_0$ is given in nm, then the Wiener process increments by definition must have units of $\sqrt{\mathrm{m}}$ and Γ, must be given in units of $\mathrm{nm}/\sqrt{\mathrm{m}}$. In (12) Γ is given in units of nm. Therefore the scaling by the length of the fibre L in $\Sigma^{'}$ is plausible.

A more compact way of writing (21), is to define the operator $\mathcal{H}$,

$$\mathcal{H}[f(x_1,x_2)] = \left[\frac{Cov\left(\Delta\lambda_1^{'}, \Delta\lambda_1^{'}\right)}{\frac{\sigma_{\lambda_1}}{m^2}}, \frac{Cov\left(\Delta\lambda_2^{'}, \Delta\lambda_2^{'}\right)}{\frac{\sigma_{\lambda_2}}{m^2}}\right] \times \begin{bmatrix} \frac{\partial^2 f(x_1,x_2)}{\partial x_1^2} & \rho\frac{\partial^2 f(x_1,x_2)}{\partial x_1 \partial x_2} \\ \rho\frac{\partial^2 f(x_1,x_2)}{\partial x_1 \partial x_2} & \frac{\partial^2 f(x_1,x_2)}{\partial x_2^2} \end{bmatrix} \begin{bmatrix} \frac{\sigma_{\lambda_1}}{m^2} \\ \\ \frac{\sigma_{\lambda_2}}{m^2} \end{bmatrix}. \quad (22)$$

Therefore the Taylor expansion of $E[G(\Delta\lambda_1^{'}, \Delta\lambda_2^{'})]$, can be written as,

$$\begin{aligned} E[G(\Delta\lambda_1^{'}, \Delta\lambda_2^{'})] \approx\ & G(\langle\Delta\lambda_1^{'}\rangle, \langle\Delta\lambda_2^{'}\rangle) + \\ & + \frac{1}{2!}\mathcal{H}\left[G(\Delta\lambda_1^{'}, \Delta\lambda_2^{'})\right]\Big|_{\substack{\Delta\lambda_1^{'} = \langle\Delta\lambda_1^{'}\rangle \\ \Delta\lambda_2^{'} = \langle\Delta\lambda_2^{'}\rangle}} + \\ & + \frac{1}{4!}\mathcal{H}\left[\mathcal{H}\left[G(\Delta\lambda_1^{'}, \Delta\lambda_2^{'})\right]\right]\Big|_{\substack{\Delta\lambda_1^{'} = \langle\Delta\lambda_1^{'}\rangle \\ \Delta\lambda_2^{'} = \langle\Delta\lambda_2^{'}\rangle}} + \\ & + \frac{1}{6!}\mathcal{H}\left[\mathcal{H}\left[\mathcal{H}\left[G(\Delta\lambda_1^{'}, \Delta\lambda_2^{'})\right]\right]\right]\Big|_{\substack{\Delta\lambda_1^{'} = \langle\Delta\lambda_1^{'}\rangle \\ \Delta\lambda_2^{'} = \langle\Delta\lambda_2^{'}\rangle}} + \cdots. \end{aligned} \quad (23)$$

III. Experimental validation

For the experimental validation of the Monte Carlo and theoretical model discussed in subsections II-B and II-C, respectively, we will use the experimentally measured ZDW fluctuations profile obtained by Mussot et al in Fig. 2 a) of [9] for a single-core single-pump FOPA. We set the correlation length to be $L_{c_1} = L_{c_2} = L_c$. We recall that for single-core single-pump FOPA the auto-correlation function is given by $R(\zeta) = \langle\delta\lambda_0(z)\delta\lambda_0(z+\zeta)\rangle$ [4] and

$$L_c = \int_0^L \frac{R(\zeta)}{R(0)}d\zeta \approx \sum_{m=\frac{N-1}{2}+1}^{N} \frac{R(\zeta_m)}{R(0)}\Delta\zeta_m, \quad (24)$$

where N is the number of points digitally obtained from the auto-correlation function. N was obtained by spline interpolation of the obtained curve of [9, Fig. 2 a)] in steps of $\Delta z = 0.1$ m and the auto-correlation function is estimated

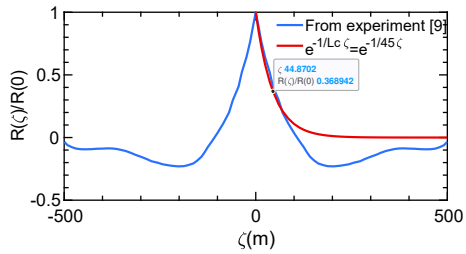

Fig. 2. Estimation of auto-correlation function. Blue and red curves are the experimentally obtained and fit of the exponential auto-correlation function with $L_c = 45$ m

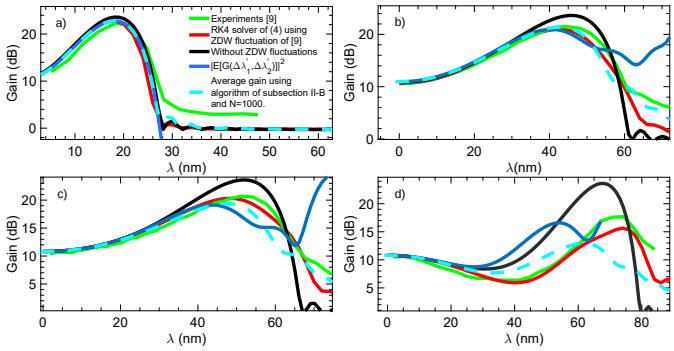

Fig. 3. Matched curves between RK4 algorithm (red) discussed in subsection II-B, average gain (blue) for ZDW fluctuations with $L_{c_1} = L_{c_2} = 39.2$ m, $\sigma_{\lambda_1} = \sigma_{\lambda_2} = \sigma = 0.33$ nm, $\gamma = 11.2$ $\mathrm{W}^{-1}\,\mathrm{km}^{-1}$, $L = 500$ m and $\rho = 1$, obtained for 4^{th} order Taylor expansion of $E[G(\Delta\lambda_1^{'}, \Delta\lambda_2^{'})]$, discussed in subsection II-C and light dashed blue curve obtained for $N = 1000$ realizations of the fibre ZDW fluctuations using Monte-Carlo simulations algorithm discussed in subsection II-B. Black curve provides the spectrum for which there is no ZDW fluctuations and green curve provides the experimentally obtained spectrum of [9, Fig. 2 b)], resultant from ZDW fluctuations obtained in [9, Fig. 2 a)]. The gain spectra are provided for a pump wavelength of a) 1555 nm and $P_p = 1.24$ W, b) 1553.3 nm and $P_p = 1.29$ W, c) 1553.2 nm and $P_p = 1.27$ W and d) 1553 nm and $P_p = 1.27$ W. To note that gain is given as the absolute value squared of G, i.e., $|G(\Delta\lambda_1, \Delta\lambda_2)|^2$. To note as well that in order to emulate single-core cases with the expression for $G(\Delta\lambda_1, \Delta\lambda_2)$ given by (19), the pump power per core in a dual-core model presented in section II must be identical to the single-core model presented in the literature related with frequency non-degenerated FOPA.

given the above-mentioned equation. Using (24) we estimate the correlation length to be $L_c \approx 39$ m. Since One can also estimate L_c, by plotting the normalized auto-correlation function $\frac{R(\zeta)}{R(0)}$, and observe the length for which $\frac{R(\zeta)}{R(0)} = e^{-1}$ as it is shown in Fig. 2. In that case $L_c \approx 45$ m and a good agreement is obtained between the experimental auto-correlation function and fit. This shows that an OU process describes reasonably well the effect of ZDW fluctuations in an optical fiber, and that ZDW fluctuations can be approximately considered to be exponentially correlated. Nonetheless we will use the value obtained with (24) for the experimental validation of the models presented in subsections II-B and II-C. This choice is justified because (24) is a more accurate approximation than just trying to fit the curve, despite no dramatic changes will be noticed if one uses the value obtained by the fit.

Fig. 3 shows the gain spectrum for a pump wavelengths 1555 nm, 1553.3 nm, 1553.2 nm and 1553 nm. In Fig. 3

$E[G(\Delta\lambda_1^{'}, \Delta\lambda_2^{'})]$, resulting from (23), provides the average assuming several realizations of the fiber (blue curve) and it is compared with its numerical analogue, i.e., a Monte Carlo simulation model (light dashed blue curve) discussed in subsection II-B, while the other curves are simulated or experimentally obtained for one fiber sample investigated in [9, Fig. 2 a) and Fig. 2 b]. To note that in order to use the models discussed in subsections II-B and II-C to emulate single-core cases, we have to assume the cores are identical, i.e., $\rho = 1$, $\sigma_{\lambda_1} = \sigma_{\lambda_2} = \sigma_\lambda = 0.33$ nm, $L_{c_1} = L_{c_2} = L_c = 39.2$ m. It is required the use of the expression given by (19) to calculate the average of the gain, i.e., $E[G(\Delta\lambda_1^{'}, \Delta\lambda_2^{'})]$ and make $C = 0$. The value of the standard deviation of ZDW fluctuations $\sigma = 0.33$ nm is obtained from Fig. 2 a) of [9]. To note that in this experimental validation, we exceptionally included loss by substituting in (19) $P_p z = P_p L_{eff}$ [32] and multiply $G(\Delta\lambda_1^{'}, \Delta\lambda_2^{'})$ by $e^{\frac{-\alpha z}{2}}$, where $L_{eff} = \frac{1-e^{-\alpha z}}{\alpha}$, and $\alpha = 0.56$ dB/km is the loss parameter. All the parameters are the same as the ones used in [9], i.e., $\beta_4 = -3.6 \times 10^{-56}$ s^4/m and $\beta_3 = 4.41 \times 10^{-41}$ s^3/m. The only exception is that we found that the average ZDW must be ≈ 1553.1 nm, while in [9] is mentioned it is ≈ 1553 nm. What makes us think that our assumption is right, is that in Fig 3 d) the gain drops immediately after a few nm after the wavelength of the pump, indicating that when the pump is at 1553 nm, the pump is indeed in the normal dispersion regime. This cannot be a result of ZDW fluctuations since close to the pump wavelength, the effect of ZDW fluctuations is negligible.

Our theoretical model discussed in section II-C given by (23) is accurate in the scenarios where the phase-mismatch is relatively small or the approximated gain function is well-behaved (avoiding large derivatives), which happens normally within the gain spectrum of the FOPA. It provides a fairly accurate prediction of what the average gain will be, while the solution of (4), using RK4 algorithm and ZDW fluctuations shown in [9] discussed in section II-B, provides a much accurate prediction of the experimentally obtained gain spectrum. We can see that for all the pump wavelengths discussed previously an accurate estimation of the most likely average gain is given, compared to the experimentally obtained gain spectrum. Finally increasing the order of the Taylor expansion will increase the accuracy of the estimation of $E[G(\Delta\lambda_1^{'}, \Delta\lambda_2^{'})]$ at higher values of λ, especially for the cases the pump is near the ZDW, such as in Figs. 3 c) and d). The phase-mismatch fluctuation resulting from ZDW fluctuations increase with λ, increasing the error of the Taylor series for higher values of λ. The derivative of the gain in order to the ZDW flutuations of core 1 and 2 will also increase with λ. Note that the remainder of a Taylor expansion is also proportional to this derivative [36]. The computation time, increases almost exponentially with the order of the Taylor expansion used and therefore we have truncated it to a 4^{th} order Taylor expansion (about 30 minutes in a desktop personal computer). Nevertheless, a 4^{th} or even a 6^{th} order Taylor expansion is likely to require much less computation time than performing Monte Carlo simulation and this is more evident for shorter correlation lengths.

One side conclusion of this section is that typical highly nonlinear fiber cores are very likely to have standard deviation of ZDW fluctuations in the order of sub-nm and longitudinal correlation lengths in the order of tenths of meters.

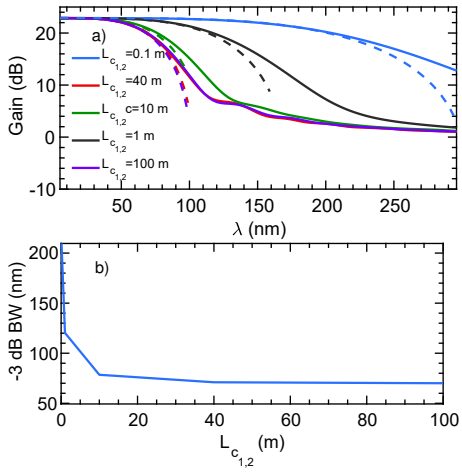

Fig. 4. a) Average gain spectrum over 1000 realizations of the fiber and b) related -3 dB BW for several values of correlation length where $L_{c_1} = L_{c_2}$. In a) dashed curves as a result of 6^{th} order Taylor expansion described by (23), solid curves provides the average gain spectrum as a result of the Monte-Carlo simulation model discussed in subsection II-B and solving (4). For all the cases plotted $C = 0.0133$ m^{-1}, $\sigma_{\lambda_1} = \sigma_{\lambda_2} = 0.5$ nm, $\rho = 1$, $P_p = 3.8$ W, $\beta_3 = 4.41 \times 10^{-41}$ s^3/m, $L = 125$ m, $\gamma = 14$ W^{-1} km^{-1} and $\beta_4 = 0$ s^4/m. The pump is located in the average ZDW, thus $\lambda_{p_1} = \lambda_{p_2} = \langle\lambda_{0_1}\rangle = \langle\lambda_{0_2}\rangle$

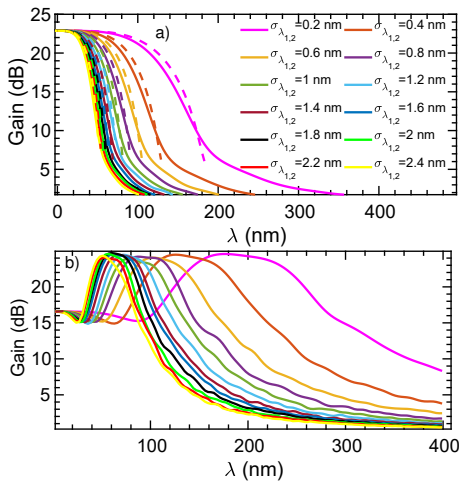

Fig. 5. a) and b) Average gain spectrum over 1000 realizations of the fiber for several values of standard deviation $\sigma_{\lambda_{1,2}}$, where we assume $\sigma_{\lambda_1} = \sigma_{\lambda_2}$. In a) $C = 0.0133$ m^{-1} $P_p = 3.8$ W, $\rho = 0$, b) $C = 0$ m^{-1}, $L = 125$ m, $\gamma = 14$ W^{-1} km^{-1} and $P_p = 7.6$ W and $\rho = 1$ (connected with single-core case). In a) dashed curves as a result of 6^{th} order Taylor expansion described by (23), solid curves provides the average gain spectrum as a result of the Monte-Carlo simulation model by simulating 1000 fiber samples, discussed in subsection II-B and solving (4). For all the cases plotted , $L_{c_1} = L_{c_2} = 10$ m, $\beta_3 = 4.41 \times 10^{-41}$ s^3/m and $\beta_4 = 0$ s^4/m. The pump is located in the average of the ZDW and therefore $\lambda_{p_1} = \lambda_{p_2} = \langle\lambda_{0_1}\rangle = \langle\lambda_{0_2}\rangle$. We omit the dash lines in b) since while the theoretical model can predict well the region where the gain is flat, it diverges for very large λ outside this region for the reasons discussed already in section III.

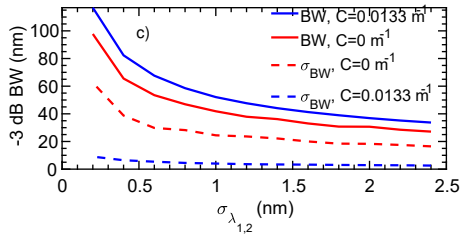

Fig. 6. Average -3 dB BW and standard deviation σ_{BW} of the -3 dB BW across the 1000 fiber realizations for several values of standard deviations $\sigma_{\lambda_{1,2}}$, where we assume $\sigma_{\lambda_1} = \sigma_{\lambda_2}$. The values of the coupling parameter are given as $C = 0.0133$ m^{-1} and $C = 0$ m^{-1} with same parameters as in Fig. 5 a) and b), respectively.

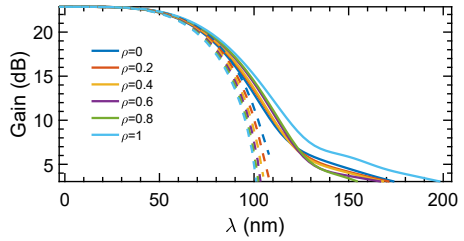

Fig. 7. Average gain spectrum over 1000 realizations of the fiber for several values of Pearson correlation coefficient ρ. In a) dashed curves as a result of 6^{th} order Taylor expansion described by (23), solid curves provides the average gain spectrum as a result of the Monte-Carlo simulation model discussed in subsection II-B and solving (4). For all the cases plotted $C = 0.0133$ m^{-1}, $\sigma_{\lambda_1} = \sigma_{\lambda_2} = 0.5$ nm, $L_{c_1} = L_{c_2} = 40$ m, $P_p = 3.8$ W, $\beta_3 = 4.41 \times 10^{-41}$ s^3/m, $L = 125$ m, $\gamma = 14$ W^{-1} km^{-1} and $\beta_4 = 0$ s^4/m. The pump is located in the average of the ZDW, thus $\lambda_{p1} = \lambda_{p2} = \langle \lambda_{0_1} \rangle = \langle \lambda_{0_2} \rangle$.

IV. The Coupled Dual-Core Fiber Optical Parametric Amplifier Case

In this section we demonstrate and discuss the results for a coupled DC-FOPA, showing in Fig. 4 the evolution of the gain spectrum and BW as a function of the correlation length. In Fig. 5 we show the evolution of the gain spectrum as a function of the standard deviation of ZDW fluctuations and in Fig. 7 the evolution as a function of the Pearson correlation coefficient. An example is provided in order to forecast the typical gain spectrum of DC-FOPA with realistic ZDW fluctuations. All the plots are computed using the models discussed in subsections II-B and II-C, using a Monte Carlo RK4 solution of (4) and (23), respectively. The Monte-Carlo model discussed in II-B, comprises simulation of 1000 different fibers each with its own ZDW fluctuations and required standard deviation and correlation length.

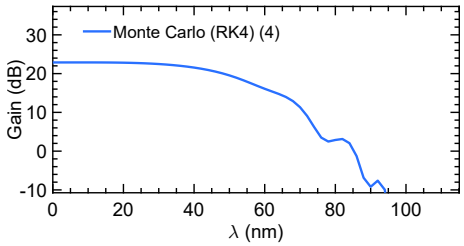

Fig. 8. Coupled DC-FOPA gain spectrum assuming ZDW fluctuations of Fig 2 a) of [9] in both cores, i.e. $\rho = 1$. For blue curve $C = 0.0034$ m^{-1}, $\sigma_{\lambda_1} = \sigma_{\lambda_2} = 0.33$ nm, $L_{c_1} = L_{c_2} = 39.2$ m, $P_p = 1.24$ W, $\beta_3 = 4.41 \times 10^{-41}$ s^3/m, $L = 500$ m, $\gamma = 11.2$ W^{-1} km^{-1}, $\alpha = 0.56$ dB/km and $\beta_4 = 0$ s^4/m. The pump is located in 1553 nm.

From Fig. 4 a) a good agreement can be appreciated between the Monte Carlo simulation model discussed in subsection II-B and theoretical model discussed in subsection II-C given by (23), for each value of correlation length. For a better agreement a higher order Taylor expansion would be required which can become computationally very expensive for large values of λ, where large values of phase-mismatch occur. In Fig. 5 a) with $C = 0.0133$ m^{-1} and b) with $C = 0$ m^{-1}, it is shown the variation of the gain spectrum with the standard deviation of fluctuations $\sigma_{\lambda_{1,2}}$. In Fig. 5 a) good agreement between the model of subsection II-B and II-C is shown. In Fig. 5 b) the case where we have used $C = 0$ and $\rho = 1$ has been presented too. As discussed in section III, this is closely related with the case of a single-core single-pump FOPA. The model developed in (23) is not suitable or it is computationally demanding if one wants to approximate accurately, for large λ and large phase-mismatch or where the approximated function $E[G(\Delta\lambda_1^{'}, \Delta\lambda_2^{'})]$ is not smooth (large derivatives). The Taylor expansion does not seem to predict correctly in this situation. However it is possible to obtain from it, qualitative information and as it can be seen in section III, it provides accurate quantitative information as well. Nonetheless, we note that the Monte Carlo simulations in Fig. 5 b) provide the typical experimental spectrum obtained in the literature [37, Fig. 6 b)] for significantly high quadratic gains, i.e., > 10 dB, which is the case of Fig. 5 b). Fig. 6 shows the -3 dB BW comparison obtained from Monte Carlo simulations comparing the BW obtained in Fig. 5 a) and b). The cases of Fig. 5 a) and b) provide a fair comparison between a coupled DC-FOPA in a) and single-core single-pump FOPA in b) where the total power used in just one core in b) is equal to the total power used and required in a) for both cores, i.e., $P_p = 3.8$ W. The case of Fig. 5 a) still has $\approx 20\%$ more BW, within the spectral region where the spectral response of the DC-FOPA is flat, than the case depicted in Fig. 5 b). Moreover, within that BW the case shown in a), has ≈ 4 times more average gain than the case depicted in b). Moreover, the variation, or standard deviation, of the spectral BW where the spectral response of the FOPA is flat, i.e., σ_{Bw}, is much higher in the single-core single-pump FOPA than in the case of the coupled DC-FOPA. Therefore the spectral response of the single-core single-pump FOPA is much more sensitive to ZDW fluctuations than the DC-FOPA.

In Fig. 7, we show the gain variation, with the Pearson correlation coefficient ρ. No significant changes occur in the gain spectrum when ρ varies. The case where the ZDW fluctuations are anti-correlated do not change this conclusion and therefore are omitted. In Fig. 8 we predict how it would be the gain spectrum of a coupled DC-FOPA if both cores have the same ZDW fluctuations given by Fig. 2 a) of [9]. This will lead to about 50 nm BW, which is impressive if we take into account the large length of the fiber , i.e, $L = 500$ m. We can compare it with the average -3 dB BW, obtained through the Monte Carlo simulation model for an identical correlation length, maximum gain and standard deviation shown in Fig. 4 b), but with $L = 125$ m. In that case we have obtained ≈ 70

nm with more than 20 dB flat spectral gain. This is expected since shorter FOPAS are likely to provide wider gain spectrum.

Notably in coupled DC-FOPA, ZDW fluctuations do not change the gain profile or damage the gain spectral flatness. For instance ZDW fluctuations damage the gain spectral flatness in single-core dual pump FOPAs [6] and in single-core single-pump FOPAs, this damage has also been observed for reasonably high quadratic gain (gain close to the pump wavelength) [37, Fig. 6 b)]. Moreover comparatively to single-core dual pump FOPA, the gain flatness is kept even in the most demanding statistical conditions, limiting BW only. The physical interpretation for this is that the maximum gain of single-core dual pump FOPA is dependent on the phase-matching condition being equal to zero. This condition is perturbed by the ZDW fluctuations leading to ripples in the gain spectrum, and eventually to a net/average phase-mismatch different than 0, on distinct wavelengths. In DC-FOPA the phase matching condition that gives the maximum gain is ruled, especially as small detuning from the pump where the gain is flat, by the balancing between the nonlinear phase-mismatch given by $\gamma P_p/2$ and $2C$, (see for example [13, Eq. 25]). Since the coupling does not fluctuate (in theory), the gain flatness is kept. On the other hand dispersion limits the amplifier BW at larger detuning from the pump which may explain why ZDW fluctuations affect mostly BW in our study.

The impact of other phenomena such as randomness of coupling parameter needs to be studied, but since the coupling parameter depends on the core radius, fluctuations in the core radius will impact the coupling parameter and will generate induced ZDW fluctuations and coupling phase fluctuations that are likely to be partially correlated. It is not clear if coupling fluctuations will be beneficial or detrimental, since the coupling is wavelength dependent and higher order terms of the coupling dispersion can be used to compensate waveguide/core dispersion. This problem will be the subject of future studies.

V. Conclusions

We conclude that ZDW fluctuations in single-/multi-core fibers is a unidimensional/multidimensional Ornstein–Uhlenbeck (OU) process, respectively. We have developed a Monte Carlo simulation model that implements a multidimensional OU process. We have also developed a theoretical model based on a Taylor approximation of the average of the gain,that is capable to accurately describe the OU process and matches the Monte Carlo simulation model results. The experimental data analysed was collected from [9] and demonstrates a correlation length of about 39 m and a standard deviation of about 0.33 nm. Thus it is expected that current highly-nonlinear fiber cores, have correlation lengths and standard deviations of that order of magnitude. Coupled DC-FOPAs present spectral gain flatness even in the most demanding statistical conditions. Compared to single-core single-pump and dual pump FOPAs they show superior resilience to fiber imperfections and unlike the former, only -3 dB BW and not maximum gain is affected by ZDW fluctuations. We conclude that coupled DC-FOPA is a serious candidate for future broadband amplification, with its unique noise properties that can deliver a broadband flat gain amplifier with potential for very low noise figures and with its stronger immunity to ZDW fluctuations as demonstrated in this work.

Acknowledgment

Marie Skłodowska-Curie Actions POLSAR (713694) is acknowledged. The following EPSRC projects funded the local Aston cluster, used in the simulations of this paper, PEACE (EP/L000091/1), PHOS (EP/S003436/1), UNLOC (EP/J017582/1) and TRANSNET (EP/R035342/1). Auro M. Perego acknowledges support from the Royal Academy of Engineering under the Research Fellowship scheme. we would like to acknowledge the voluntary effort of reviewers, especially reviewer 1, but also reviewer 2 for the very detailed review reports provided and the time voluntarily given in reviewing this technical work. Matlab Files with scripts and data extracted from figures are available under reasonable request.

References

[1] P. A. Andrekson and M. Karlsson, "Fiber-based phase-sensitive optical amplifiers and their applications," *Adv. Opt. Photon., AOP*, vol. 12, no. 2, pp. 367–428, Jun. 2020.

[2] C. B. Gaur, F. Ferreira, V. Gordienko, V. Ribeiro, and N. J. Doran, "Demonstration of improved performance provided by fopa for extended pon in burst-mode operation," in *45th European Conference on Optical Communication (ECOC 2019)*, 2019, pp. 1–3.

[3] C. B. Gaur, F. Ferreira, V. Gordienko, V. Ribeiro, Á. D. Szabó, and N. J. Doran, "Experimental comparison of fiber optic parametric, raman and erbium amplifiers for burst traffic for extended reach PONs," *Opt. Express, OE*, vol. 28, no. 13, pp. 19 362–19 373, Jun. 2020.

[4] M. Karlsson, "Four-wave mixing in fibers with randomly varying zero-dispersion wavelength," *J. Opt. Soc. Am. B, JOSAB*, vol. 15, no. 8, pp. 2269–2275, Aug. 1998.

[5] P. Velanas, A. Bogris, and D. Syvridis, "Impact of dispersion fluctuations on the noise properties of fiber optic parametric amplifiers," *J. Lightwave Technol., JLT*, vol. 24, no. 5, p. 2171, May 2006.

[6] F. Yaman, Q. Lin, S. Radic, and G. P. Agrawal, "Impact of dispersion fluctuations on dual-pump fiber-optic parametric amplifiers," *IEEE Photonics Technol. Lett.*, vol. 16, no. 5, pp. 1292–1294, May 2004.

[7] V. Ribeiro, V. Gordienko, C. Gaur, and N. Doran, "The impact of zero-dispersion wavelength fluctuations in > 110 nm fiber optical raman+parametric amplification," in *2018 European Conference on Optical Communication (ECOC)*, 2018, pp. 1–3.

[8] M. Farahmand and M. de Sterke, "Parametric amplification in presence of dispersion fluctuations," *Opt. Express*, vol. 12, no. 1, pp. 136–142, Jan. 2004.

[9] A. Mussot, E. Lantz, A. Durecu-Legrand, C. Simonneau, D. Bayart, T. Sylvestre, and H. Maillotte, "Zero-dispersion wavelength mapping in short single-mode optical fibers using parametric amplification," *IEEE Photonics Technol. Lett.*, vol. 18, no. 1, pp. 22–24, Jan. 2006.

[10] E. Myslivets and S. Radic, "Spatially resolved measurements of the chromatic dispersion in fibers," *J. Lightwave Technol.*, vol. 33, no. 3, pp. 597–608, Feb. 2015.

[11] B. Jaramillo Ávila, J. M. Torres, R. d. J. León-Montiel, and B. M. Rodríguez-Lara, "Optimal crosstalk suppression in multicore fibers," *Sci. Rep.*, vol. 9, no. 1, p. 15737, Oct. 2019.

[12] J. S. Y. Chen, S. G. Murdoch, R. Leonhardt, and J. D. Harvey, "Effect of dispersion fluctuations on widely tunable optical parametric amplification in photonic crystal fibers," *Opt. Express*, vol. 14, no. 20, pp. 9491–9501, Oct 2006. [Online]. Available: http://opg.optica.org/oe/abstract.cfm?URI=oe-14-20-9491

[13] V. Ribeiro, M. Karlsson, and P. Andrekson, "Parametric amplification with a dual-core fiber," *Opt. Express*, vol. 25, no. 6, pp. 6234–6243, Mar. 2017.

[14] V. Ribeiro, A. Lorences-Riesgo, P. Andrekson, and M. Karlsson, "Noise in phase-(in)sensitive dual-core fiber parametric amplification," *Opt. Express*, vol. 26, no. 4, pp. 4050–4059, 2018.

[15] V. Ribeiro, A. D. Szabó, A. M. Rocha, C. B. Gaur, A. A. I. Ali, Y. Quiquempois, A. Mussot, G. Bouwmans, and N. Doran, "Parametric amplification and wavelength conversion in dual-core highly nonlinear fibers," *Journal of Lightwave Technology*, pp. 1–8, 2022.

[16] V. Ribeiro and A. M. Perego, "Theory of parametric amplification in coupled lossy waveguides," in *Conference on Lasers and Electro-Optics*. Optical Society of America, 2022, p. JTh3A.12.

[17] A. D. Szabó, V. Ribeiro, C. B. Gaur, A. A. I. Ali, A. Mussot, Y. Quiquempois, G. Bouwmans, and N. J. Doran, "Dual-polarization c+l-band wavelength conversion in a twin-core highly nonlinear fibre," *OFC 2021 Virtual conference, Paper MB5.4*, 2021.

[18] V. Ribeiro and A. M. Perego, "Parametric amplification in lossy nonlinear waveguides with spatially dependent coupling," *Opt. Express*, vol. 30, no. 10, pp. 17 614–17 624, 2022.

[19] M. Shi, V. Ribeiro, and A. M. Perego, "Parametric amplification based on intermodal four-wave mixing between different supermodes in coupled-core fibers," *Opt. Express*, vol. 31, pp. 9760–9768, 2023.

[20] ——, "On the resilience of dual-waveguide parametric amplifiers to pump power and phase fluctuations," *Applied Physics Letters*, vol. 122, no. 10, 03 2023.

[21] S. Trillo, S. Wabnitz, G. I. Stegeman, and E. M. Wright, "Parametric amplification and modulational instabilities in dispersive nonlinear directional couplers with relaxing nonlinearity," *J. Opt. Soc. Am. B*, vol. 6, no. 5, pp. 889–900, 1989.

[22] M. Deserno, "How to generate exponentially correlated gaussian random numbers," *Department of Chemistry and Biochemistry UCLA, USA*, 2002.

[23] R. Singh, D. Ghosh, and R. Adhikari, "Fast bayesian inference of the multivariate ornstein-uhlenbeck process," *Physical Review E*, vol. 98, no. 1, p. 012136, 2018.

[24] M. Koshiba, K. Saitoh, K. Takenaga, and S. Matsuo, "Multi-core fiber design and analysis: coupled-mode theory and coupled-power theory," *Opt. Express*, vol. 19, no. 26, pp. B102–B111, Dec 2011. [Online]. Available: http://opg.optica.org/oe/abstract.cfm?URI=oe-19-26-B102

[25] T. Hayashi, T. Sasaki, E. Sasaoka, K. Saitoh, and M. Koshiba, "Physical interpretation of intercore crosstalk in multicore fiber: effects of macrobend, structure fluctuation, and microbend," *Opt. Express*, vol. 21, no. 5, pp. 5401–5412, Mar 2013. [Online]. Available: http://opg.optica.org/oe/abstract.cfm?URI=oe-21-5-5401

[26] J. A. P. Morgado and A. V. T. Cartaxo, "Correlation and power distribution of intercore crosstalk field components of polarization-coupled weakly coupled single-mode multicore fibres," *Photonics*, vol. 8, no. 6, 2021. [Online]. Available: https://www.mdpi.com/2304-6732/8/6/191

[27] S. Finch, "Ornstein-uhlenbeck process," 2004.

[28] G. Wetzstein, D. Lanman, M. Hirsch, and R. Raskar, "Tensor displays: Compressive light field synthesis using multilayer displays with directional backlighting," *ACM Trans. Graph.*, vol. 31, no. 4, jul 2012. [Online]. Available: https://doi.org/10.1145/2185520.2185576

[29] P. Chen, "Modelling the stochastic correlation," Master's thesis, KTH, Mathematical Statistics, 2016.

[30] A. Mecozzi, "Parametric amplification and squeezed-light generation in a nonlinear directional coupler," *Opt. Lett.*, vol. 13, no. 10, pp. 925–927, Oct 1988. [Online]. Available: https://opg.optica.org/ol/abstract.cfm?URI=ol-13-10-925

[31] Z. Tong, C. Lundström, P. A. Andrekson, C. J. McKinstrie, M. Karlsson, D. J. Blessing, E. Tipsuwannakul, B. J. Puttnam, H. Toda, and L. Grüner-Nielsen, "Towards ultrasensitive optical links enabled by low-noise phase-sensitive amplifiers," *Nat. Photonics*, vol. 5, no. 7, pp. 430–436, Jun. 2011.

[32] M. Karlsson, J. Schröder, P. Zhao, and P. A. Andrekson, "Analytic theory for parametric gain in lossy integrated waveguides," in *2021 Conference on Lasers and Electro-Optics (CLEO)*, 2021, pp. 1–2.

[33] E. Gobet and G. Matulewicz, "Parameter estimation of ornstein–uhlenbeck process generating a stochastic graph," *Statistical Inference for Stochastic Processes*, vol. 20, no. 2, pp. 211–235, 2017.

[34] G. E. Uhlenbeck and L. S. Ornstein, "On the theory of the brownian motion," *Phys. Rev.*, vol. 36, pp. 823–841, Sep 1930. [Online]. Available: https://link.aps.org/doi/10.1103/PhysRev.36.823

[35] H. Benaroya, S. M. Han, and M. Nagurka, *Probability models in engineering and science*. CRC press, 2005, vol. 192.

[36] G. B. Folland, "Higher-order derivatives and taylor's formula in several variables," *Preprint*, pp. 1–4, 2005.

[37] V. Gordienko, M. F. C. Stephens, A. E. El-Taher, and N. J. Doran, "Ultra-flat wideband single-pump raman-enhanced parametric amplification," *Opt. Express*, vol. 25, no. 5, pp. 4810–4818, Mar. 2017.